The International Journal of Advanced Manufacturing Technology (2024) 134:191–204
https://doi.org/10.1007/s00170-024-14099-1

ORIGINAL ARTICLE

Study on the surface layer properties of magnesium alloys after impulse shot peening

Skoczylas Agnieszka[1] · **Zaleski Kazimierz**[1] · **Ciecieląg Krzysztof**[1] · **Matuszak Jakub**[1]

Received: 25 March 2024 / Accepted: 2 July 2024 / Published online: 18 July 2024

Abstract

Shot peening is a commonly used method of finishing machine elements in the manufacturing process. One variation of shot peening is the impulse shot peening. This paper presents the influence of impulse shot peening technological conditions on the surface roughness (parameters Ra and Rt), topography, and microhardness. The FEM was used to determine the S11 stresses. In the experiment and simulation tests, AZ31 and AZ91HP magnesium alloy samples were used. Variable parameters in the impulse shot peening process were impact energy E (15–185 mJ), ball diameter d (3–15 mm), and impact density j (3–44 mm^{-2}). As a result of the tests carried out, it was found that after impulse shot peening, the surface topography is change, microirregularities are flattened, and numerous depressions are formed, which can be potential lubrication pockets. The 2D surface roughness parameters for most impulse shot peening conditions are lower than for the pre-machining. The roughness parameters for magnesium alloy AZ91HP are lower than for AZ31. This is most likely due to the lower elongation A. The microhardness after impulse shot peening increased by 20 to 87 HV. As a result of FEM of the impulse shot peening, compressive stresses S11 were created in the surface layer. The depth of occurrence of S11 stresses is from 1.5 to 3.5 mm, and their values for the AZ91HP magnesium alloy samples are 10 to 25% lower than for the AZ31 alloy samples. The most favorable results of the tested properties of the surface layer were obtained for $E = 100$ mJ, $d = 10$ mm, and $j = 11$ mm^{-2}. The abstract serves both as a general introduction to the topic and as a brief, non-technical summary of the main results and their implications.

Keywords Magnesium alloy · Impulse shot peening · Surface roughness · Surface topography · Microhardness · FEM simulation · Stress S11

1 Introduction

Shot peening is one of the finishing methods in which the shot peening elements exert a dynamic impact on the treated surface. A widely used method of shot peening is jet shot peening, which is characterized by the fact that the shot peening elements are ejected from the peening device and hit the workpieces [1, 2]. Steel [3], glass [4], and ceramic [5] balls are used as shot peening elements. Another variation of shot peening is vibratory shot peening. In the vibratory shot peening process, workpieces and shot peening elements (usually steel balls) are placed in a working chamber which performs oscillating motion [6, 7].

In both jet and vibratory shot peening processes, the peening elements move in a "disordered" manner; therefore, it is difficult to determine parameters such as the impact energy of the shot peening elements and the number of impacts per unit area (impact density). These parameters can however

Zaleski Kazimierz, Ciecieląg Krzysztof, and Matuszak Jakub contributed equally to this work.

✉ Skoczylas Agnieszka
a.skoczylas@pollub.pl

Zaleski Kazimierz
k.zaleski@pollub.pl

Ciecieląg Krzysztof
k.ciecielag@pollub.pl

Matuszak Jakub
j.matuszak@pollub.pl

[1] Department of Production Engineering, Faculty of Mechanical Engineering, Lublin University of Technology, 36 Nadbystrzycka Street, 20-618, Lublin, Poland

be determined in impulse shot peening, in which the shot peening elements hit the workpiece with a known energy. The distances between successive dimples of hits can also be determined, which makes it possible to calculate impact density [8, 9].

Shot peening is mainly used to improve the properties of the surface layer of workpieces. As a result of shot peening, the geometric surface structure is increased, the surface layer is hardened, and compressive residual stresses are induced [10–12]. The practical result of changes induced in the properties of the surface layer by shot peening is an increased fatigue life of the workpiece [13, 14]. Shot peening also affects wear resistance [15, 16] and corrosion resistance [17]. Changes in the adhesive properties of treated surfaces as a result of shot peening were also observed, which led to increased strength of adhesive joints [18].

Surface layer properties that are favorable in terms of service life can also be obtained by burnishing. Burnishing involves impacting the surface of the workpiece with a smooth and hard burnishing element, with the force of this impact maintained at an approximately constant value [19, 20].

Effects similar to those obtained by shot peening and burnishing can also be produced by brushing. In brushing, a brush with metal or ceramic fibers is rotated at high speed to exert impact on the treated surface. In addition to changing the properties of the surface layer, brushing results in the removal of post-machining burrs and in the shaping of edges of produced parts [21, 22].

Shot peening, burnishing, and brushing are used as finishing processes for, among others, magnesium alloy components. Owing to their properties such as low density, low coefficient of friction, and ability to damp vibration, these alloys are an attractive construction material. The main areas of application of magnesium alloys include the aviation and automotive industries. Shot peening and burnishing increase the service life of components made of magnesium alloys and also make it possible to eliminate finishing, during which there is a risk of chip ignition [23].

Previous studies have mainly studied the effect of jet shot peening on the surface layer properties and service life of magnesium alloys. Wang et al. found that cold spraying shot peening of magnesium alloy AZ91D caused a significant increase in the microhardness of the surface layer and its wear resistance [24]. A study [25] investigated the effect of shot peening materials (glass, Ce-ZrO_2, Zirblast B30) on the surface roughness, microhardness distribution, residual stresses, and fatigue life of magnesium alloy AZ80. The impact of Almen intensity on the properties of the surface layer and fatigue life of this alloy was studied in [26–28]. Fouad and El Batanouny conducted a comparative study of various surface treatments (burnishing, shot peening) on the wear rate of magnesium alloy AZ31 [29].

An important functional property of magnesium alloys is their corrosion resistance. Research by Liu et al. showed that shot peening resulted in a significant improvement in the corrosion resistance of magnesium alloy AZ31, while for the AZ91 alloy, the improvement in this resistance was insignificant [30]. Mhaede et al. studied the effect of shot peening on the surface roughness, microhardness distribution, and corrosion properties of the biocompatible magnesium alloy AZ31 samples coated with dicalcium phosphate dihydrate [31]. A study [32] investigated the effect of severe shot peening on the surface roughness, microhardness and residual stress distribution, fatigue properties, and corrosion resistance of magnesium alloy AZ31.

Favorable changes in surface layer properties were obtained as a result of ultrasonic shot peening treatment and cavitation peening. The ultrasonic shot peening treatment of magnesium alloy AZ31 caused a very large increase in the microhardness of the surface layer, which increased the wear resistance and reduced the friction coefficient [33]. Fatigue tests of ZK60 samples after ultrasonic peening treatment (UPT) showed a beneficial effect of this treatment on the residual stress distribution and fatigue strength. Changes in crack initiation sites were observed in the samples after UPT [34]. Zagar et al. found that cavitation peening of heat treatable magnesium alloy AZ80A resulted in an increase in the microhardness of the surface layer and in the formation of compressive residual stresses, as well as led to a several-fold increase in the Ra parameter of surface roughness [35].

Burnishing generally produces a lower surface roughness compared to that obtained by shot peening. Research by Jagadeesh and Setti allowed the determination of the ball burnishing parameters for magnesium alloy Ze41A that ensured the lowest surface roughness [36]. A study [37] investigated the influence of burnishing force, feed rate, the number of passes, and medium type in the ball burnishing process for magnesium alloy AZ91D on the roughness of the machined surface of this material. The results of the study investigating the stereometric structure of magnesium alloy AZ91 after slide diamond burnishing were reported in [38]. On the other hand, the use of deep surface rolling as a treatment for magnesium alloy AZ91 made it possible to obtain a very large increase in hardness [39].

A study [40] presents the results of surface roughness tests of AZ91HP and AZ31 magnesium alloys after brushing with brushes with steel and brass fiber. The effectiveness of deburring and shaping the edges of brushed objects was also studied.

Previous studies on shot peening magnesium alloys have focused on jet and vibratory shot peening. The technological parameters determined in these types of shot peening processes relate to shot peening devices such as air pressure and the distance of the nozzle from the workpiece (in jet shot peening), as well as the amplitude and frequency of

vibrations of the vibrator (in vibratory shot peening). Parameters directly related to the shot peening process, such as impact energy and impact density, can be determined via impulse shot peening. The aim of this study is to determine the effect of impulse shot peening process parameters on the surface roughness and microhardness distribution and stress S11 of magnesium alloys AZ31 and AZ91HP.

2 Research methodology

In this study, samples of AZ31 and AZ91HP magnesium alloys were used. Their chemical compositions defined based on the quality control certificate and selected properties are listed in Table 1. The Young's modulus value for both alloys is approx. 45 GPa.

Classified as a wrought alloy, AZ31 is one of the most widely used alloys in mechanical engineering. AZ31 has good tensile strength and good plasticity, and it is also well weldable. This material is suitable for rolling, stamping, and extrusion [41]. The AZ31 alloy is designed to work at room temperature or at temperatures up to 100 °C [42].

AZ91HP is a casting alloy. It is characterized by good strength and low ductility (elongation of about 2–3%) [43]. The AZ91HP alloy has high purity and corrosion resistance due to a low content of impurities such as Fe, Ni, and Cu. It is used, among others, for Audi's five-speed transmission castings.

Rectangular samples with the dimensions of $4 \times 15 \times 100$ mm were used in the tests. Milling was applied as a pre-machining treatment. The milling operation was conducted using a three-blade folding face milling cutter with a diameter of 25 mm. The following machining parameters were used: cutting speed ($v_c = 71$ m/min), feed per tooth ($f_z = 0.01$ mm/tooth), and cutting depth ($a = 1$ mm).

Impulse shot peening was performed on a specially designed test stand. A regular shot peening method was used; i.e., traces were placed next to each other with the assumed step (x) (which is schematically shown in Fig. 1). In detail, this method of applying traces was described in [9]. The shot peening stand consisted of a replaceable head that allowed for changing the diameter of the ball-shaped burnishing element (d). The cam mechanism and the spring made it possible to change impact energy (E). The sample was mounted on a CNC table performing feed motion. The feed speed affected the value of shot peening density (j) (number of hits per unit area, formula 1). The CNC table moved according to the assumed program.

$$j = \frac{1}{x^2}, \left[\mathrm{mm}^{-2}\right] \tag{1}$$

where: x - distance between dimples.The applied technological parameters of impulse shot peening are listed in Table 2.

Surface roughness and topography measurements were made using a T800 RC120-400 device from Hommel-Etamic. The measurements were made in accordance with EN ISO 25178–2: 2022–06. The analyzed surface roughness parameters were Ra (the arithmetic average of profile height deviations from the mean line) and Rt (the total height of the profile). These surface roughness parameters were selected for analysis owing to the fact that they are widely used in engineering practice. The area of the scanned surface was 1.5×1.5 mm.

The microhardness of the surface layer before and after impulse shot peening was measured by the Vickers method using a Leco LM 700 at microhardness tester. The measurements were made on the surface, assuming an indenter weight of 100 g (HV 0.1).

The shot peening process was analyzed numerically using the explicit function of the Abaqus CAE software, taking into account surface contact. The Johnson–Cook model was applied in the FEM simulation, taking into consideration factors such as temperature, stresses, material strengthening, and plastic deformation speed to reproduce the real machining process. For each shot peening element, mass and initial velocity were assigned to reflect impact energy. The diameters and depths of the indentations obtained by numerical modelling were compared to those of the real indentations resulting from the impact of the shot peening elements on the machined surface. C3D8R type elements were used for the numerical model. A $10 \times 10 \times 4$ mm sample was used in the simulation. In

Table 1 Chemical composition and selected properties of AZ31 and AZ91HP magnesium alloys according the PN-EN 1753:2020–01 and material card

Grade	Chemical compositions (wt%)								
	Cu	Mn	Mg	Zn	Si	Fe	Al	Ni	Other
AZ31	–	0.25	Rest	0.81	0.01	0.003	2.90	0.0004	0.3
AZ91HP	0.002	0.22	Rest	0.66	0.016	0.002	8.91	0.001	Be – 0.001
Grade	Properties								
	R_m (MPa)		$R_{p0.2}$ (MPa)		A (%)		Hardness (HB)		
AZ31	250–255		110–150		17–21		64		
AZ91HP	190–240		150–170		3.5		82		

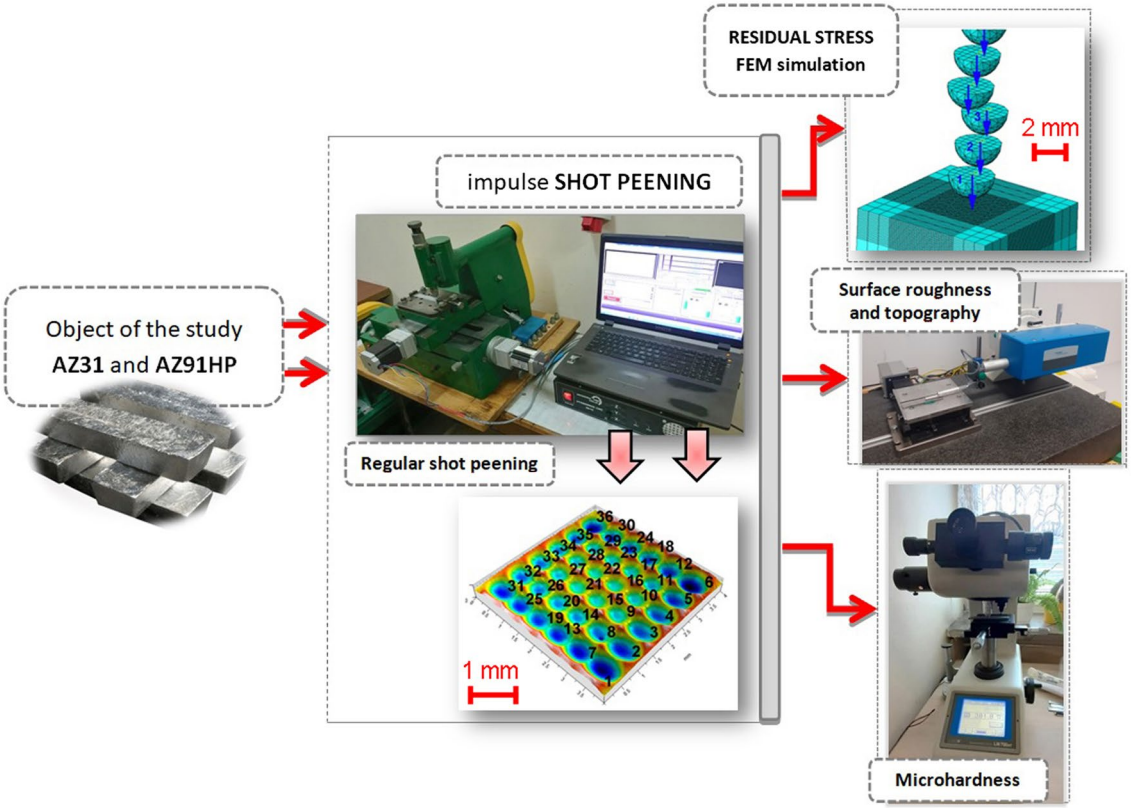

Fig. 1 Research methodology for testing selected properties of the surface layer of elements made of magnesium alloys AZ31 and AZ91HP

Table 2 Technological parameters of impulse shot peening for magnesium alloys AZ31 and AZ91HP

No	Impact energy E (mJ)	Ball diameter d (mm)	Distance between dimples x (mm)	Impact density j (mm^{-2})
1	15	10	0.30	11
2	100			
3	185			
4	100	3		
5		15		
6		10	0.15	44
7			0.60	3

the area of direct contact between the shot peening element and the workpiece, the mesh was reduced to 0.1 mm. The mesh contained 68,992 finite elements, with the number of nodes equal to 74,727. R3D4 (476 elements) and R3D3 (2616 elements) types of element were used to model the ball-shaped peening element. The S11 stress state in the surface layer after the shot peening process was analyzed. Figure 2 shows the arrangement of reference points representing the location of impact. The influence of impact energy (adopted at levels: 15; 100; 185mJ), the diameter of the shot peening element (adopted at levels 3; 10; 15 mm) and the distance between the dimples (0.15; 0.30 and 0.60 mm) were analyzed. The shot peening elements were distributed in the assembly module so that they hit one after the other. To optimize the simulation, the impact time of all 36 shot peening elements was determined for each of set parameters, which was specified in the step module of the Abaqus program.

Figure 3a shows the visualization of 36 impacts according to the applied methodology (shot peening element diameter and speed, distance between the dimples). Figure 3b shows the real view of a sample after 36 impacts.

Stress diagrams S11 from the FEM simulation were determined as the average value of three cross-section paths drawn perpendicularly to the surface, as shown in Fig. 4.

3 Results

3.1 Surface topography

The pattern of microirregularities visible on the surface after milling is similar to the pattern characteristic of machined surfaces, which results from the geometric-kinematic mapping of the tool corner in the workpiece (Fig. 5a). The microirregularities visible on the surface are plastically deformed

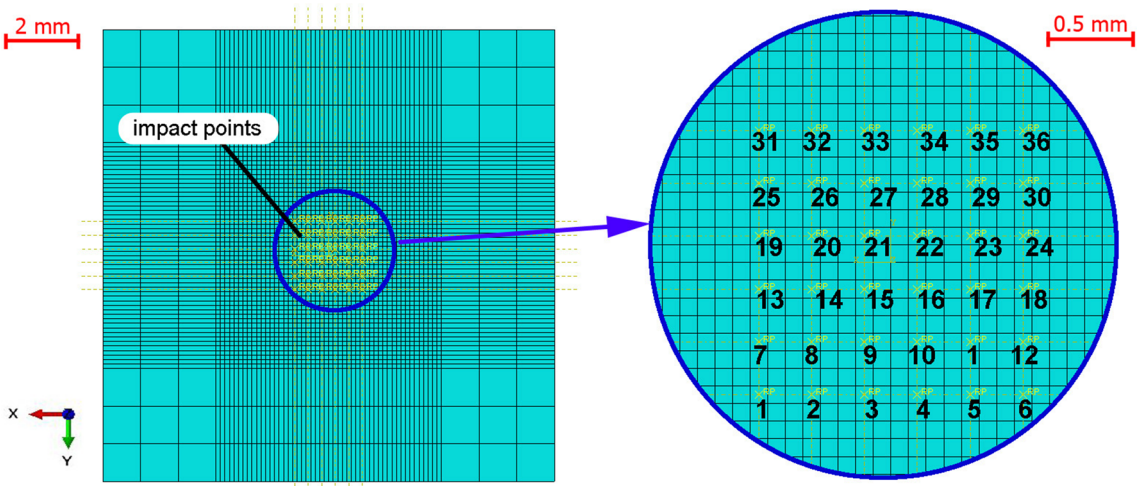

Fig. 2 View of the arrangement of reference points representing the location of impact

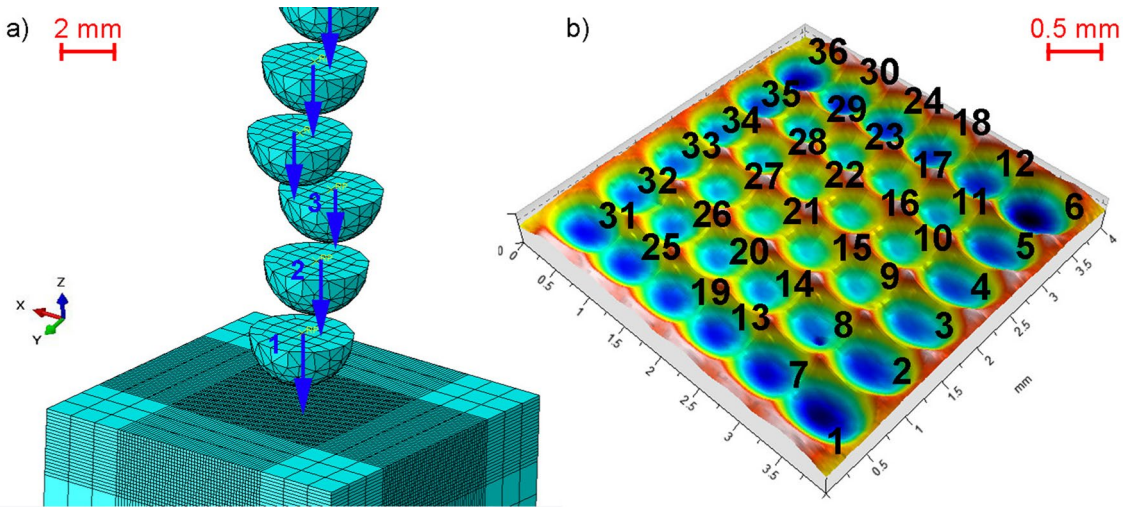

Fig. 3 FEM simulation of the shot peening process: **a** visualization of 36 impacts according to the applied methodology and **b** real view of a sample

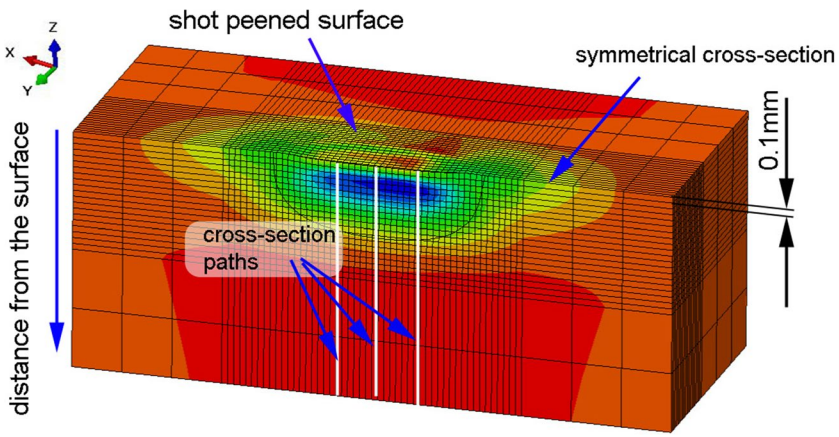

Fig. 4 Method of determination the averaged S11 stress distribution based on three paths

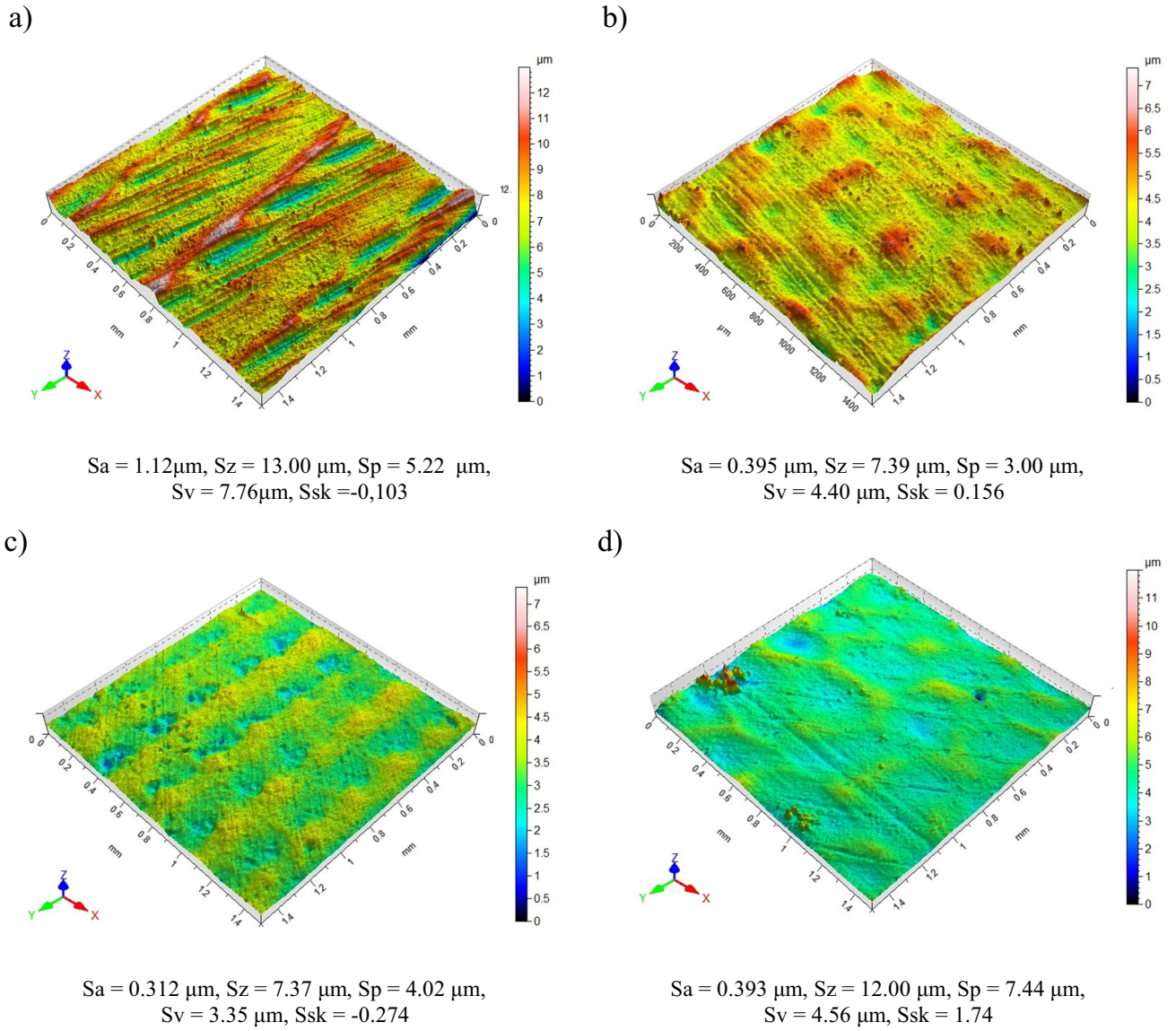

Fig. 5 Surface topography of AZ31 magnesium alloy samples: **a** after milling; **b** after impulse shot peening ($E = 10$ mJ, $j = 11$ mm^{-2}, $d = 10$ mm); **c** after impulse shot peening ($E = 100$ mJ, $j = 11$ mm^{-2}, $d = 10$ mm); **d** after impulse shot peening ($E = 185$ mJ, $j = 11$ mm.$^{-2}$, $d = 10$ mm)

as a result of friction between the working surfaces of the tool and the machined surface. They have a similar height of peaks and depth of depressions. The resulting surface topography should be classified as a unidirectional structure.

On the surface after impulse shot peening (Fig. 5b–d), there are visible depressions resulting from the impact of the ball on the surface of the sample. The resulting depressions have a different shape than after milling. They are characterized by a spherical shape, which may mean that the surface after impulse shot peening will have a better lubricant retention capacity than the surface after milling. It can be seen that for the impact energy $E = 185$ mJ, the surface is deformed to a greater extent (deeper valleys and higher elevations). After impulse shot peening, the skewness parameter Ssk changes. The use of $E = 100$ mJ, $d = 10$ mm, and $j = 11$ mm^{-2} causes the Ssk value to decrease in relation to the value after milling (Fig. 5c).

An analysis of the effect of the shot-peened material on the obtained topography (Fig. 6) demonstrates that depressions of smaller depth and height are formed on the surface of the AZ91HP alloy sample. The resulting system of microirregularities for the AZ31 alloy is more ordered than that obtained for the AZ91HP alloy, which may indicate a different nature of deformation in pulse shot peening for this type of material. The AZ31 alloy is characterized by a greater elongation A and lower hardness, which favors the formation

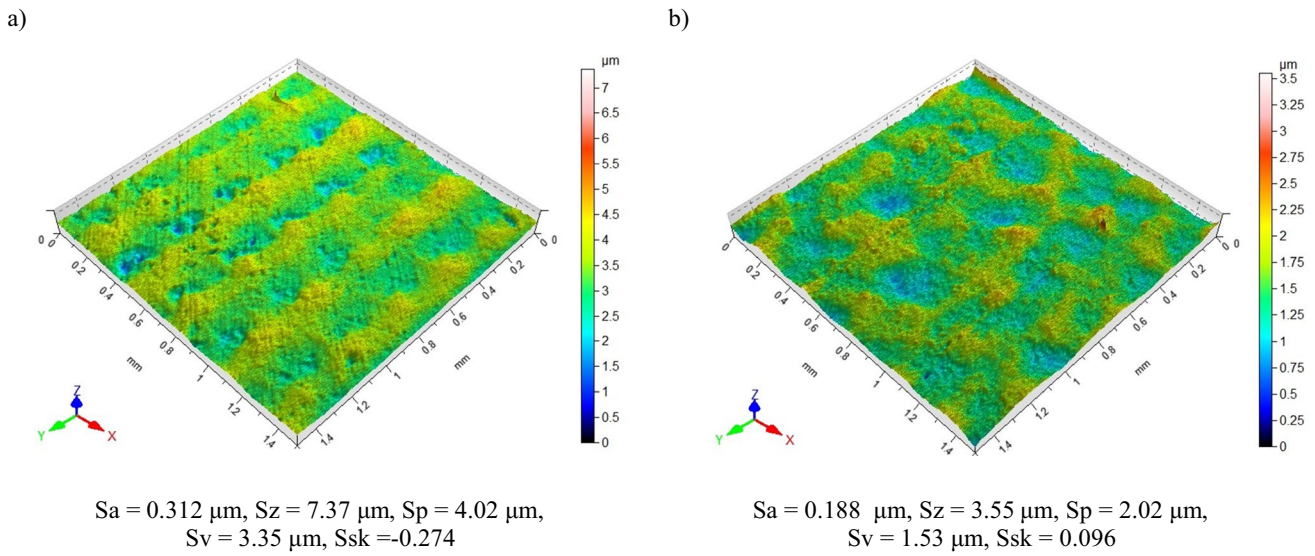

Fig. 6 Surface topography of AZ31 (**a**) and AZ91HP (**b**) magnesium alloy samples after impulse shot peening ($E = 100$ mJ, $j = 11$ mm.$^{-2}$, $d = 10$ mm)

of uniform traces characterized by a similar depth and the formation of flash next to the trace of impulse shot peening.

3.2 Surface roughness

Figure 7 shows the influence of impact energy on the surface roughness parameters Ra (Fig. 7a) and Rt (Fig. 7b). For the impact energy values used in the experiment, the Ra and Rt values are lower than after the pre-treatment. The use of a higher impact energy value ($E > 15$ mJ) causes an increase in the degree of deformation, which consequently leads to a slight decrease in the surface roughness parameters Ra and Rt (for AZ31). The application of an impact energy value of $E = 185$ mJ causes relatively insignificant changes in the surface roughness parameter Ra compared to the value obtained for $E = 100$ mJ. The roughness reduction at $E = 100$ mJ is related to a greater levelling of microirregularities after milling than that observed for $E = 15$ mJ. At $E = 185$ mJ, the knocking out of microirregularities due to impact is more noticeable. Changes in the surface roughness in the range of impact energy $E = 100$–185 mJ are more noticeable for the Rt parameter. The obtained values of the parameters Ra and Rt as a function of impact energy for magnesium alloy AZ91HP are lower than for AZ31, which may be due to a lower value of elongation A.

The use of balls with a larger diameter ($d = 10$–15 mm) causes a smaller degree of plastic deformation than that

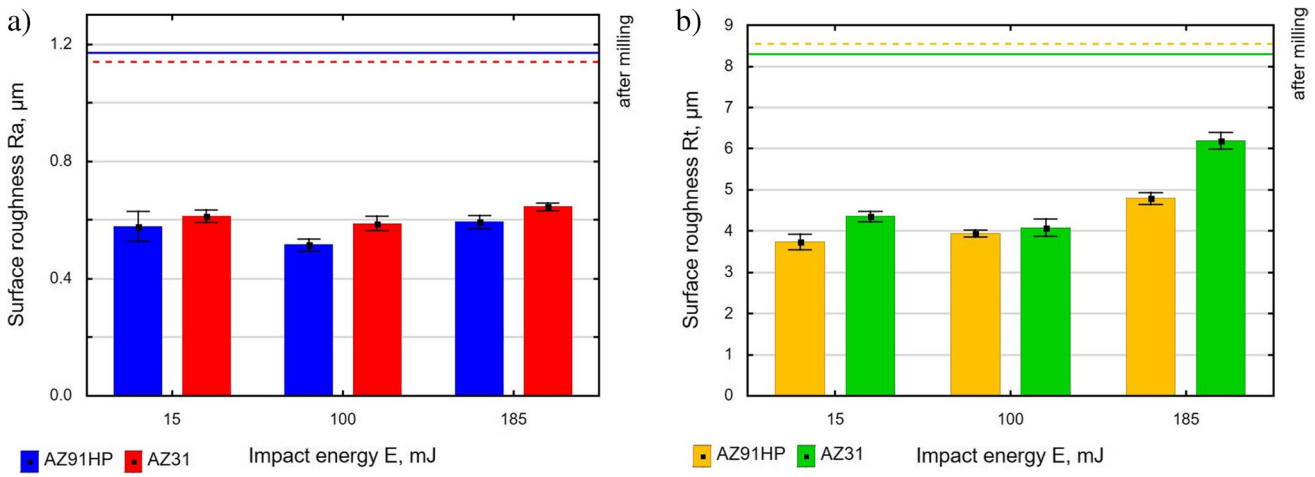

Fig. 7 Effect of impact energy on surface roughness parameters Ra (**a**) and Rt (**b**) ($d = 10$ mm, $j = 11$ mm.$^{-2}$)

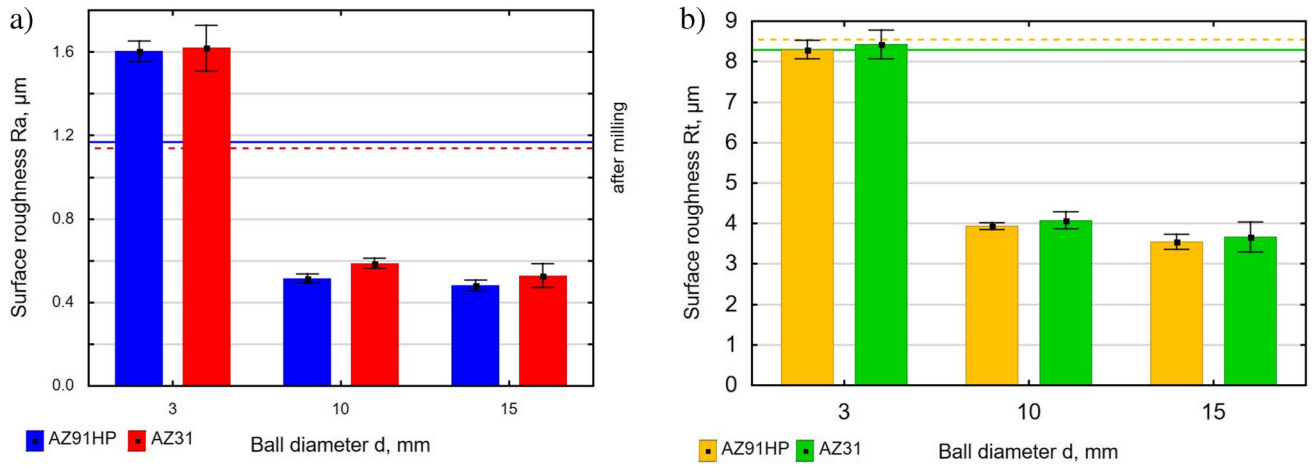

Fig. 8 Effect of ball diameter on surface roughness parameters Ra (**a**) and Rt (**b**) ($E = 100$ mJ, $j = 11$ mm.$^{-2}$)

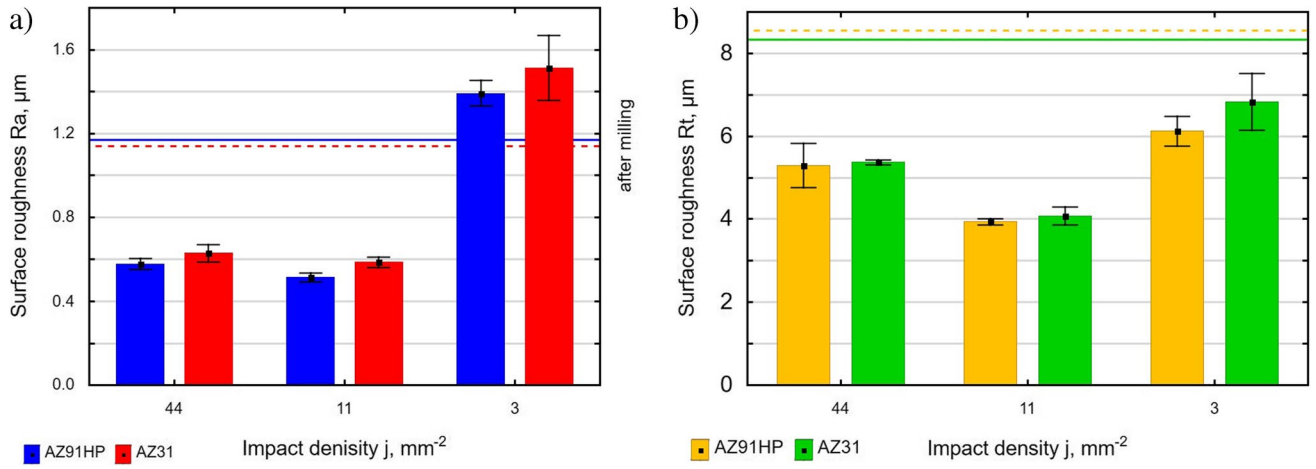

Fig. 9 Effect of impact density on surface roughness parameters Ra (**a**) and Rt (**b**) ($E = 100$ mJ, $d = 10$ mm)

observed for the ball with a diameter of $d = 3$ mm. The lower degree of deformation causes a decrease in the values of the analyzed roughness parameters Ra and Rt (Fig. 8). The use of a ball with a diameter of $d = 3$ mm contributes to an increase in the tested roughness parameters in relation to their values after milling. This should be explained by the fact that for the ball with $d = 3$ mm, the contact surface is smaller, which causes an increase in unit pressures and, consequently, generates greater surface irregularities.

An increase in the distance between the traces of impact (x) causes a decrease in the peening density (Fig. 9) and thus a decrease in the degree of surface coverage. In effect, there is uneven deformation of the impulse shot-peened surface, which is conducive to an increase in the Ra and Rt roughness parameters. For the range $j = 11$–44 mm^{-2}, there is no visible effect of peening density on the analyzed surface roughness parameters. A state of saturation can be observed.

3.3 Microhardness

The effect of impact energy (E), shot peening ball diameter (d), and shot peening density (j) on surface microhardness is shown in Figs. 10, 11, and 12. An analysis of the microhardness of the surface after impulse shot peening demonstrates that for the AZ91HP alloy samples, the microhardness increased by 30 to 87 HV, while for the AZ31 alloy, by approx. 20 to 70 HV, relative to the value achieved after milling. The microhardness of AZ91HP after impulse shot peening is higher than that of AZ31.

An increase in the impact energy (Fig. 10) causes more intensive plastic deformation of the material, which results in an increased microhardness of the surface. For the AZ91HP and AZ31 alloy samples, a linear increase in microhardness was obtained as a function of impact energy (Fig. 10).

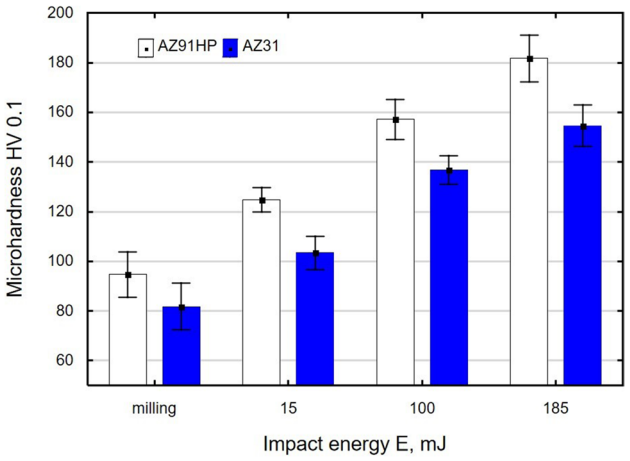

Fig. 10 Effect of impact energy E on surface microhardness ($d = 10$ mm, $j = 11$ mm.$^{-2}$)

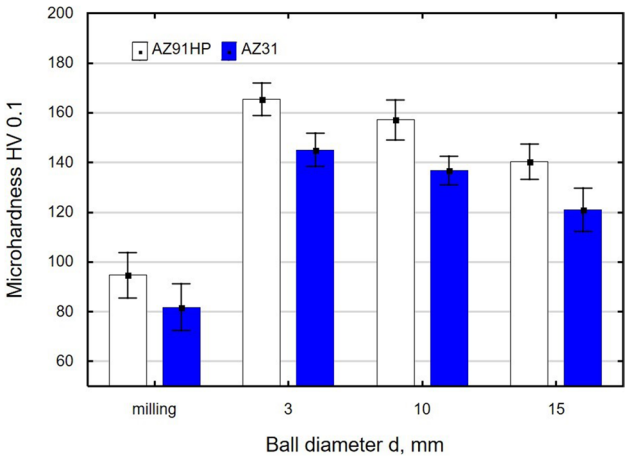

Fig. 11 Effect of shot peening ball diameter d on surface microhardness ($E = 100$ mJ, $j = 11$ mm.$^{-2}$)

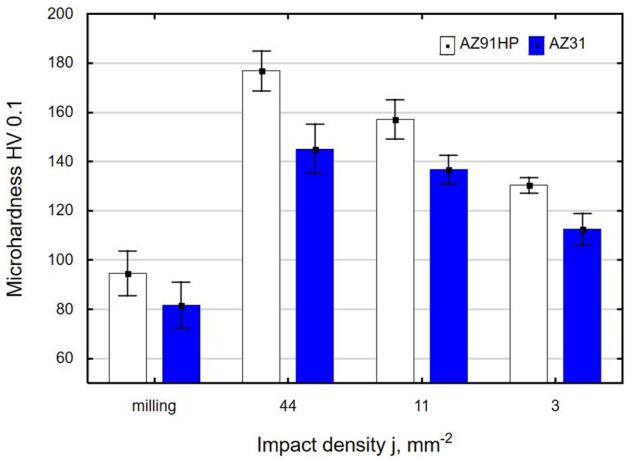

Fig. 12 Effect of impact density j on surface microhardness ($E = 100$ mJ, $d = 10$ mm)

The use of a ball with a larger diameter causes a decrease in unit pressures due to an increased area of indentation, which—in turn—leads to a decrease in the microhardness of the AZ91HP and AZ31 magnesium alloy samples (Fig. 11). These changes are the most noticeable for the diameters $d = 10$–15 mm for both magnesium alloys.

The increase in the distance between the traces corresponds to a decrease in the impact density (j). The traces after impulse shot peening are located at a greater distance, which leads to uneven deformation of the surface and, consequently, to a decrease in microhardness (Fig. 12). An increase in microhardness as a function of impact density for the AZ31 alloy is more noticeable in the range of $j = 11$–3 mm^{-2}, while for AZ91HP, it is more noticeable in the whole range of the peening density parameter values tested in the experiment.

3.4 Residual stress

Figures 13, 14, and 15 show the effect of impact energy, ball diameter, and impact density on the distribution of stresses S11 in the surface layer of elements made of magnesium alloys AZ91HP (Figs. 13a, 14a, and 15a) and AZ31 (Figs. 13b, 14b, and 15b). After impulse shot peening, compressive stresses occur in the surface layer. The distribution of stresses S11 for both materials as a function of the tested parameters is similar. The only differences can be observed for the maximum absolute value of the compressive stresses and their depth. Regardless of the impulse shot peening conditions for the AZ91HP alloy samples, the compressive stresses occur at a greater depth from the surface compared to the AZ31 alloy samples. Higher stress values were obtained for the AZ31 alloy samples than for the AZ91HP alloy. The S11 stress values for the AZ31 magnesium alloy samples are 10 to 25% higher than those for the AZ91HP alloy samples.

An increase in the impact energy (Fig. 13) causes both an increase in the absolute value of stresses S11 and the depth of their location. It can also be seen that for both materials, the depth of occurrence of the maximum absolute value of compressive stresses is similar.

The use of a ball with a larger diameter increases the depth of location of compressive stresses S11 (Fig. 14). For smaller diameter balls, there is a greater absolute value of stress. The use of a ball with a diameter of $d = 10$ mm or $d = 15$ mm does not cause significant differences in the value and depth of the compressive stresses.

An increase in the impact density results in more complete deformation of the surface of the impact shot-peened samples made of the AZ91HP and AZ31 alloys. Consequently, there is an increase in the absolute value of the

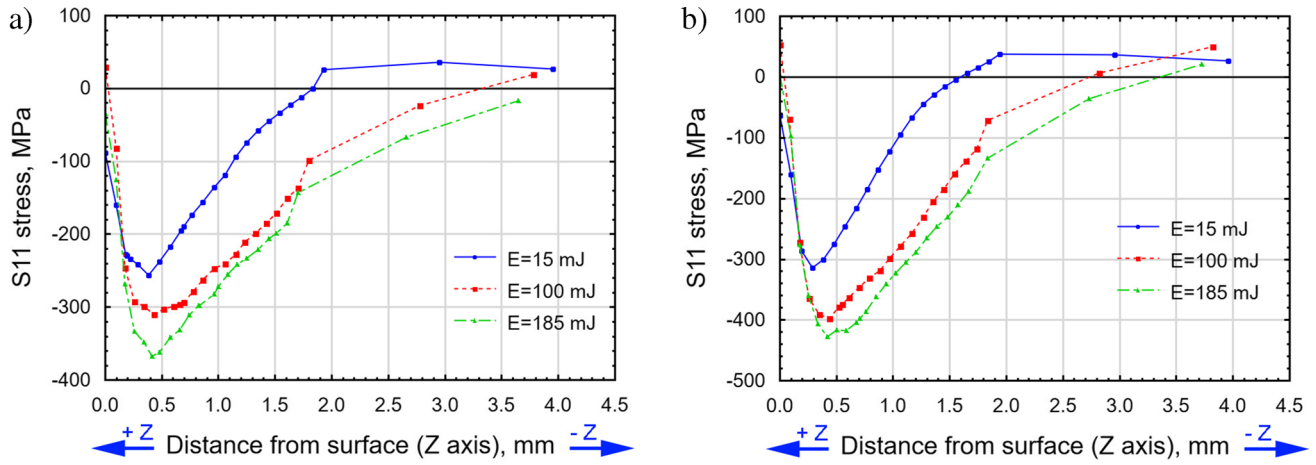

Fig. 13 Distribution of residual stresses as a function of distance from the surface of AZ91HP (**a**) and AZ31 (**b**) samples after impulse shot peening with a variable impact energy ($d = 10$ mm, $j = 11$ mm.$^{-2}$)

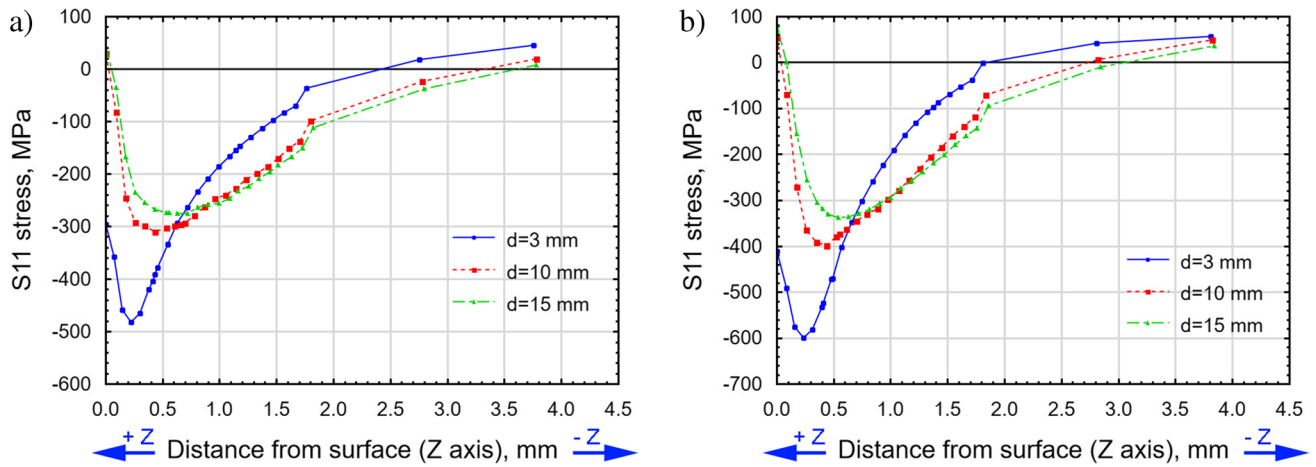

Fig. 14 Distribution of residual stresses as a function of distance from the surface of AZ91HP (**a**) and AZ31 (**b**) samples after impulse shot peening with a variable ball diameter ($E = 100$ mJ, $j = 11$ mm.$^{-2}$)

maximum compressive stresses and the depth of their location (Fig. 15).

4 Discussion

The analysis of the works presented in the literature review shows that magnesium alloys are the subject of many studies. The use of magnesium alloys in industry enforces the need to study them thoroughly and to know the properties of the surface layer especially after various finishing. Improving the quality of the surface layer can be achieved by impulse shot peening. An analysis of the obtained results confirms that impulse shot peening induces changes in the surface layer properties of the elements made of magnesium alloys AZ31 and AZ91HP.

Specifically, the surface topography and roughness of the impulse shot-peened samples are changed. The values of the Ra and Rt parameters for the AZ91HP and AZ31 alloys are lower than the results obtained via conventional shot peening (CSP) and several shot peening (SSP) of the AZ31 alloy reported in [30, 32]. Also, the roughness values obtained in this study for the AZ31 magnesium alloy are lower than those obtained for the shot-peened samples in [44]. Favorable surface roughness values (lower than those reported in [45]) may contribute to improved fatigue resistance and higher corrosion resistance [24]. The shot peening process analyzed in this work is classified as a dynamic burnishing method. Compared to static burnishing methods, the Ra values of impulse shot-peened samples are up to 845% higher than those of the WE43 magnesium alloy subjected to ball burnishing in the MQL

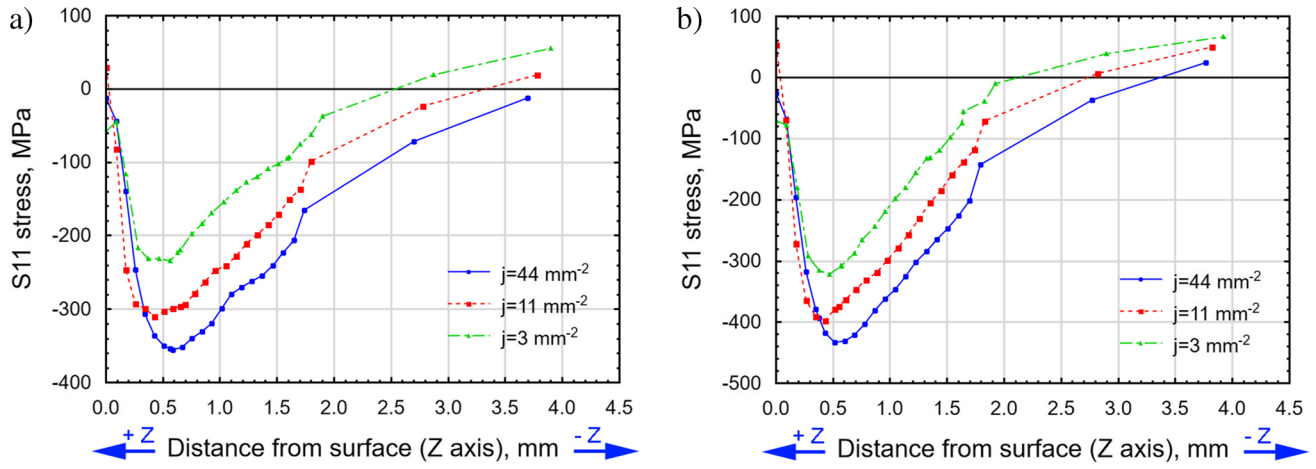

Fig. 15 Distribution of residual stresses as a function of distance from the surface of AZ91HP (**a**) and AZ31 (**b**) samples after impulse shot peening with a variable impact density ($E = 100$ mJ, $d = 10$ mm)

environment (Ra ranged from 0.187 to 0.396 µm) [46], while the ball-burnished AZ91D magnesium alloy samples had the Ra parameter ranging from 0.336 to 0.718 µm [47]. Comparing the obtained values of the Ra parameter for the AZ91HP magnesium alloy with the results from [47] and for the biodegradable AZ31B magnesium alloy [48], it should be noted that lower surface roughness was obtained for some of the technological parameters of impulse shot peening. An analysis of the impact of the medium (ball diameter) used in impulse shot peening demonstrates that the ball diameter exerts the same impact on roughness parameters as that observed in shot peening of magnesium alloy AZ80 reported in [25]. Regarding the relationship between density (j) and surface roughness parameters for magnesium alloys AZ31 and AZ91HP, the effect is similar to that produced by impulse shot peening of aluminum alloys EN AW 7075 and EN AW 2017A and nickel alloy, as reported in the author's previous studies [8, 9]. An analysis of shape parameters (Ssk and Sku) showed that the most favorable properties in terms of abrasive wear resistance ($Ssk < 0$ and $Sku > 3$) were obtained for the impulse shot peening process of AZ31 alloy elements conducted using $E = 100$ mJ, $j = 11$ mm^{-2}, and $d = 10$ mm. The obtained values of Ssk and Sku will probably contribute to improved contact conditions of the friction pair elements by reducing their plasticity indices and accelerating volume wear reduction. Low Ssk and high Sku surfaces can act as "traps" capturing wear particles [49–51].

The strain energy transferred during impulse shot peening to the magnesium alloy elements causes microstructural changes and, consequently, changes their microhardness. The experimental results demonstrate that higher microhardness was obtained for the AZ91HP alloy than for AZ31. This finding is in line with the results of previous studies on burnishing [36, 39] and shot peening for these engineering materials [24, 30, 31, 33]. The microhardness increase for the two tested materials is similar to the values obtained after several shot peening [30]. The highest similarity to the results presented in [30] can be observed for the impulse shot peening of the AZ91HP and AZ31 samples conducted using $j = 3$ mm^{-2}. A comparison of the microhardness increase in AZ91HP to the results obtained after deep rolling [39] reveals that the changes in microhardness are at a similar level; but after deep rolling, they occur at greater depths, while in relation to a study [47] (maximum microhardness HV = 102), the microhardness values obtained after impulse shot peening are higher (HV 0.1 max = 181).

The microstructural changes induce changes in the state of residual stresses. As a result of impulse shot peening, compressive residual stresses were generated in the surface layer. Regardless of the processing conditions, the stress values obtained for the AZ31 alloy samples and their depth are higher than those produced by warm shot peening treatments [52], while the residual stresses are higher for both AZ31 and AZ91HP than those obtained for Mg Ze41A after ball burnishing [53]. A comparison of the obtained stress S11 values with those reported in previous studies [9] reveals that the FEM stress values obtained for the AZ91HP and AZ31 alloy samples are lower than those obtained for the EN AW 7075 alloy. However, the use of impulse shot peening generates a greater depth of compressive stress in AZ91HP and AZ31 than that observed for EN AW 7075. This means that the fatigue crack initiation location shifts from the surface to the subsurface layers. These changes will most likely delay crack nucleation and propagation [54]. As a result of the crack initiation location displacement, the resistance of the workpiece to fatigue wear will probably increase.

A comparison of the obtained residual stresses and microhardness for the AZ91HP and AZ31 magnesium alloys reveals that their values are higher for the AZ91HP alloy. The observed differences most likely depend on the value of relative elongation. For the AZ91HP magnesium alloy, the relative elongation is approximately 5 times smaller compared to AZ31. This means that the material is less susceptible to deformation, so the energy transferred during impacts causes greater strains in the subsurface zones and is not transferred "deeper" into the workpiece. This causes microstructural changes and defect formation, which leads to a greater increase in the microhardness of AZ91HP compared to AZ31 and, consequently, induces changes in the values of residual stresses.

Summing up the results, it should be stated that impulse shot peening of magnesium alloy objects yields comparable or even lower values of surface roughness parameters than those obtained by ball burnishing. At the same time, the microhardness increase is at a similar level to that observed after several shot peening or deep rolling. The values and depths of the residual stresses in the AZ31 alloy are greater than after warm shot peening treatments, and their values for the impulse shot-peened AZ31 and AZ91HP samples are higher than those induced by ball burnishing. The results allow us to conclude that even though impulse shot peening is a dynamic burnishing method, it makes it possible to obtain favorable, operationally satisfactory properties of the surface layer. It should also be stated that the work is distinguished by a systematic and comprehensive approach to the analyzed issue. Previous work has in most cases been limited to the analysis of one input factor. This work expands the research area by allowing to obtain results for various input factors under constant test conditions on two magnesium alloys AZ31 and AZ91HP, so commonly used in mechanical engineering.

5 Conclusion

Based on the results obtained from the experimental tests and the simulation of the impulse shot peening process for elements made of magnesium alloys AZ91HP and AZ31, the following conclusions can be drawn:

a) After impulse shot peening, the surface topography is changed; numerous depressions on the surface are visible, and they can be potential lubrication pockets.
b) The analyzed 2D (Ra and Rt) and 3D surface roughness parameters for magnesium alloy AZ91HP are lower than for AZ31. As far milling (pre-treatment), the Ra and Rt parameters are lower for most impulse shot peening conditions.
c) The microhardness of the AZ91HP alloy increased by 30 to 87 HV, while for the AZ31 alloy, by 20 to 70 HV in relation to the value after milling.
d) In the surface layer after impulse shot peening, compressive stresses can be observed; the values of which for the AZ91HP magnesium alloy samples are 10 to 25% lower than for the AZ31 alloy samples. The depth of the compressive residual stresses ranges from 1.5 to 3.5 mm, which allows us to assume that the location of fatigue crack initiation will be displaced, when compared to that obtained for the EN AW 7075 aluminum alloy samples after impulse shot peening [9].

Author contribution All authors contributed to the study conception and design. Material preparation, data collection, and analysis were performed by all authors. The first draft of the manuscript was written by Agnieszka Skoczylas, Kazimierz Zaleski, and Jakub Matuszak, and all authors commented on previous versions of the manuscript. All authors read and approved the final manuscript.

Funding This work was supported by Lublin University of Technology, Poland, under research grant nos. FD-20/IM-5/107, FD-20/IM-5/071, and FD-20/IM-5/016.

Declarations

Conflict of interest The authors declare no competing interests.

References

1. Bao L, Li K, Zheng J, Zhang Y, Zhao B (2022) Surface characteristics and stress corrosion behavior of AA 7075–T6 aluminum alloys after different shot peening processes. Surf Coat Technol 440:128481. https://doi.org/10.1016/j.surfcoat.2022.128481
2. Swietlicki A, Szala M, Walczak M (2022) Effects of shot peening and cavitation peening on properties of surface layer of metallic materials – a short review. Materials 15(7):2476. https://doi.org/10.3390/ma15072476
3. Okolo B, Perez Willard F, Hawecker J, Gerthsen D, Wanner A (2007) Focused ion beam study of the effects of shot peening on the subsurface microstructure of normalized pearlitic steel. J Mater Process Technol 183:160–164. https://doi.org/10.1016/j.jmatprotec.2006.09.037
4. Qin Z, Li B, Zhang H, Wilfried TYA, Gao T, Xue H (2022) Effects of shot peening with different coverage on surface integrity and

fatigue crack growth properties of 7B50-T7751. Eng Fail Anal 133:106010. https://doi.org/10.1016/j.engfailanal.2021.106010
5. Chen G, Jiao Y, Tian T, Zhang X, Li Z, Zhou W (2014) Effect of wet shot peening on Ti-6Al-4V alloy treated by ceramics beads. Trans Nonferrous Metals Soc China 24:690–696. https://doi.org/10.1016/S1003-6326(14)63112-5
6. Canals L, Badreddine J, McGillivray B, Miao HY, Levesque M (2019) Effect of vibratory peening on the sub-surface layer of aerospace materials Ti-6Al-4V and E-16NiCrMo13. J Mater Process Technol 264:91–106. https://doi.org/10.1016/j.jmatprotec.2018.08.023
7. Alcaraz JY II, Zhang J, Nagalingam AP, Gopasetty SK, Toh BL, Gopinath A, Ahluwalia K, Ang MGW, Yeo SH (2022) Numerical modeling of residual stresses during vibratory peening of a 3-stage Blisk – a multi-scale discrete element and finite element approach. J Mater Process Technol 299:117383. https://doi.org/10.1016/j.jmatprotec.2021.117383
8. Skoczylas A, Zaleski K, Zaleski R, Gorgol M (2021) Analysis of surface properties of nickel alloy elements exposed to impulse shot peening with the use of positron annihilation. Materials 14:7328. https://doi.org/10.3390/ma14237328
9. Matuszak J, Zaleski K, Skoczylas A, Ciecieląg K, Kęcik K (2021) Influence of semi – random and regular shot peening on selected surface layer properties of aluminum alloy. Materials 14:7620. https://doi.org/10.3390/ma14247620. (**Personal communication**)
10. Chen M, Liu H, Wang L, Zhu K, Xu Z, Jiang C (2018) Ji, V: Evaluation of the residual stress and microstructure character in SAF 2507 duplex stainless steel after multiple shot peening process. Surf Coat Technol 344:132–140. https://doi.org/10.1016/j.surfcoat.2018.03.012
11. Bucior M, Galda L, Stachowicz F, Zielecki W (2016) The effect of technological parameters on intensity of shot peening process of 51CrV4 steel. ActaMechanica et Automatica 10(3):213–217. https://doi.org/10.1515/ama-2016-0032
12. Zaleski K, Skoczylas A, Ciecieląg K (2020) The investigations of the surface layer properties of C45 steel after plasma cutting and centrifugal shot peening. In: Królczyk GM, Niesłony P, Królczyk J (eds.) Industrial Measurements in Machining, Lecture Notes in Mechanical Engineerig, pp. 172–185 Springer
13. Klotz T, Delbergue D, Bocher P, Lévesque M, Brochu M (2018) Surface characteristics and fatigue behavior of shot peened Inconel 718. Int J Fatigue 110:10–21. https://doi.org/10.1016/j.ijfatigue.2018.01.005
14. Kubit A, Bucior M, Zielecki W, Stachowicz F (2016) The impact of heat treatment and shot peening on the fatigue strength of 51CrV4 steel. Procedia Struct Integr 2:3330–3336. https://doi.org/10.1016/j.prostr.2016.06.415
15. Das T, Erdogan A, Kursuncu B, Maleki E, Unal O (2020) Effect of severe vibratory peening on microstructural and tribological properties of hot rolled AISI 1020 mild steel. Surf Coat Technol 403:126383. https://doi.org/10.1016/j.surfcoat.2020.126383
16. Nagit G, Slatineau L, Dodun O, Mihalache AM, Ripanu MI, Hrituc A (2022) Influence of some microchanges generated by different processing methods on selected tribological characteristics. Micromachines 13(1):29. https://doi.org/10.3390/mi13010029
17. Walczak M, Szala M (2021) Effect of shot peening on the surface properties, corrosion and wear performance of 17–4PH steel produced by DMLS additive manufacturing. Arch Civil Mech Eng 21(4):157. https://doi.org/10.1007/s43452-021-00306-3
18. Rudawska A, Zaleski K, Miturska I, Skoczylas A (2019) Effect of the application of different surface treatment methods on the strength of titanium alloy sheet adhesive lap joints. Materials 12:4173. https://doi.org/10.3390/ma12244173
19 Kalisz J, Żak K, Wojciechowski S, Gupta MK, Krolczyk GM (2021) Technological and tribological aspects of milling – burnishing process of complex surfaces. Tribol Int 155:106770. https://doi.org/10.1016/j.triboint.2020.106770
20. Kowalik M, Trzepieciński T, Kukiełka L, Paszta P, Maciąg P, Legutko S (2021) Experimental and numerical analysis of the depth of the strengthened layer on shafts resulting from roller burnishing with roller braking moment. Materials 14(19):5844. https://doi.org/10.3390/ma14195844
21. Kulisz M, Zagórski I, Matuszak J, Kłonica M (2020) Properties of the surface layer after trochoidal milling and brushing: experimental and artificial neural network simulation. Appl Sci 10(1):1–26. https://doi.org/10.3390/app10010075
22. Matuszak J (2022) Comparative analysis of the effect of machining with wire and ceramic brushes on selected properties of the surface layer of EN AW – 7075 aluminium alloy. Adv Sci Tech Res J 16(2):50–56. https://doi.org/10.12913/22998624/146211
23. Zagórski I, Kuczmaszewski J (2018) Temperature measurements in the cutting zone, mass, chip fragmentation and analysis of chip metallography images during AZ31 and AZ91HP magnesium alloy milling. Aircr Eng Aerosp Technol 90(3):496–505. https://doi.org/10.1108/AEAT-12-2015-0254
24. Wang HT, Yao HL, Zhang MX, Bai XB, Yi ZH, Chen QY, Ji GC (2019) Surface nanocrystallization treatment of AZ91D magnesium alloy by cold spraying shot peening process. Surf Coat Technol 374:485–492. https://doi.org/10.1016/j.surfcoat.2019.04.093
25. Zhang P, Lindemann J, Leyens C (2010) Shot peening on the high-strength wrought magnesium alloy AZ80 – effect of peening media. J Mater Process Technol 210:445–450. https://doi.org/10.1016/j.jmatprotec.2009.10.005
26. Zhang P, Lindemann J (2005) Influence of shot peening on high cycle fatigue properties of the high-strength wrought magnesium alloy AZ80. Scr Mater 52:485–490. https://doi.org/10.1016/j.scriptamat.2004.11.003
27. Wang C, Tao X, Sun K, Wang S, Li K, Deng H (2023) On the sensitivity of the three-dimensional random representative finite element model of multiple shot impacts to the SP-induced stress field, Almen intensity, and surface roughness. Int J Adv Manuf Technol 125(5–6):2549–2567. https://doi.org/10.1007/s00170-023-10892-6
28. Qian W, Huang S, Yin X, Xie L (2022) Simulation analysis with randomly distributed multiple projectiles and experimental study of shot peening. Coatings 12(11):1783. https://doi.org/10.3390/coatings12111783
29. Fouad Y, El Batanouny M (2011) Effect of surface treatment on wear behavior of magnesium alloy AZ31. Alex Eng J 50:19–22. https://doi.org/10.1016/j.aej.2011.01.003
30. Liu C, Zheng H, Gu X, Jiang B, Liang J (2019) Effect of severe shot peening on corrosion behavior of AZ31 and AZ91 magnesium alloys. J Alloy Compd 770:500–506. https://doi.org/10.1016/j.jallcom.2018.08.141
31. Mhaede M, Pastorek F, Hadzima B (2014) Influence of shot peening on corrosion properties of biocompatible magnesium alloy AZ31 coated by dicalcium phosphate dihydrate (DCPD). Mater Sci Eng C 39:330–335. https://doi.org/10.1016/j.msec.2014.03.023
32. Bagherifard S, Hickey DJ, Fintova S, Pastorek F, Fernandez- Pariente I, Bandini M, Webster TJ, Guagliano M (2018) Effects of nanofeatures induced by severe shot peening (SSP) on mechanical and cytocompatibility properties of magnesium alloy AZ31. Acta Biomater 66:93–108. https://doi.org/10.1016/j.actbio.2017.11.032
33. Zhang J, Jian Y, Zhao X, Meng D, Pan F, Han Q (2021) The tribological behavior of a surface – nanocrystallized magnesium alloy AZ31 sheet after ultrasonic shot peening treatment. J Magnes Alloys 9:1187–1200. https://doi.org/10.1016/j.jma.2020.11.012

34. Chen Y, Liu F, Wang C, Liu Y, Wang Q (2022) Effect of ultrasonic peening treatment on the fatigue behaviors of a magnesium alloy up to very high cycle regime. J Magnes Alloys 10:614–626. https://doi.org/10.1016/j.jma.2021.07.028
35. Zagar S, Soyama H, Grum J, Sturm R (2022) Surface integrity of heat treatable magnesium alloy AZ80A after cavitation peening. J Mater Technol 17:2098–2107. https://doi.org/10.1016/j.jmrt.2022.01.156
36. Jagadeesh GV, Setti SG (2019) An experimental study on the surface finish of ball burnished magnesium (rare earth base) alloy. Mater Today: Proc 18:4711–4716. https://doi.org/10.1016/j.matpr.2019.07.457
37. Cagan SC, Pruncu CI, Buldum BB (2020) An investigation into ball burnishing process of magnesium alloy on CNC lathe using different environments. J Magnes Alloys 8:1061–1070. https://doi.org/10.1016/j.jma.2020.06.008
38. Korzynski M, Zarski T (2016) Slide diamond burnishing influence on the stereometric structure of an AZ91 alloy. Surf Coat Technol 307:590–595. https://doi.org/10.1016/j.surfcoat.2016.09.045
39. Luo X, Tan Q, Mo N, Yin Y, Yang Y, Zhuang W, Zhang M (2019) Effect of deep surface rolling on microstructure and properties of AZ91 magnesium alloy. Trans Nonferrous Metals Soc China 29:1424–1429. https://doi.org/10.1016/S1003-6326(19)65049-1
40. Matuszak J, Zaleski K (2014) Edge states after wire brushing of magnesium alloys. Aircr Eng Aerosp Technol Int J 86(4):328–335. https://doi.org/10.1108/AEAT-09-2012-0155
41. Dziubińska A, Gontarza A, Dziedzic K (2016) Qualitative research of AZ31 magnesium alloy aircraft brackets produced by a new forging method. Aircr Eng Aerosp Technol 61:1003–1008. https://doi.org/10.1515/amm-2016-0171
42. Wu Y, Liu J, Deng B, Ye T, Li Q, Zhou X, Zhang H (2020) Microstructure, texture and mechanical properties of AZ31 magnesium alloy fabricated by high strain rate biaxial forging. Materials 13(14):3050. https://doi.org/10.3390/ma13143050
43. Dziadoń A (2012) Magnesium and its alloys. Independent Section Publishing House of the Kielce University of Technology, Kielce, [in Polish]
44. Haghighi O, Amini K, Gharav F (2020) Effect of shot peening operation on the microstructure and wear behavior of AZ31 magnesium alloy. Prot Met Phys Chem Surf 56(1):164–168. https://doi.org/10.1134/S2070205120010098
45. Soyama H, Kuji C, Liao Y (2023) Comparison of the effects of submerged laser peening, cavitation peening and shot peening on the improvement of the fatigue strength of magnesium alloy AZ31. J Magnes Alloys 11(5):15529–1607. https://doi.org/10.1016/j.jma.2023.04.004
46. Cagan SC, Tasci U, Prunce CI, Bostan B (2023) Investigation of the effects of eco-friendly MQL system to improve the mechanical performance of WE43 magnesium alloys by the burnishing process. J Braz Soc Mech Sci Eng 45:22. https://doi.org/10.1007/s40430-022-03925-w
47. Buldum BB, Cagan SC (2018) Study of ball burnishing process on the surface roughness and microhardness of AZ91D alloy. Exp Tech 42:233–241. https://doi.org/10.1007/s40799-017-0228-8
48. Uddin MS, Hall C, Hooper R, Charrault E, Murphy P, Santos V (2018) Finite element analysis of surface integrity in deep ball-burnishing of a biodegradable AZ31B Mg alloy. Metals 8(2):136. https://doi.org/10.3390/met8020136
49. Wieczorowski M, Cellary A, Chajda J (2003) A guide to measuring surface unevenness, that is about surface roughness and more. Printing and Publishing Department M-Druk, Poland, Poznań [in Polish]
50. Sedlacek M, Podgornik B, Vizitin J (2009) Influence of surface preparation on roughness parameters, friction and wear. Wear 266:482–487
51. Dzierwa A, Gałda L, Tupaj M, Dudek K (2020) Investigation of wear resistance of selected materials after slide burnishing process. Eksploat iNiezawodn Maint Reliab 22:432–439. https://doi.org/10.17531/ein.2020.3.5
52. Perala LB, Zafra A, Bagherifard S, Guagliano M, Fernández-Pariente I (2020) Effect of warm shot peening treatments on surface properties and corrosion behavior of AZ31 magnesium alloy. Surf Coat Technol 401:126582. https://doi.org/10.1016/j.surfcoat.2020.126285
53. Jagadeesh GV, Srinivasu GS (2022) Experimental investigation and estimation of compressive residual stress of ball burnished rare earth based magnesium alloy. Proceedings of the institution of mechanical engineers, part e: journal of process mechanical engineering 238(1). https://doi.org/10.1177/095440892211441
54. Maximov JT, Anchev AV, Dunchev VP, Ganev N, Duncheva GV, Selimov KF (2017) Effect of slide burnishing basic parameters on fatigue performance of 2024–T3 high-strength aluminium alloy. Fatigue Fract Eng Mater Struct 40:1893–1904. https://doi.org/10.1111/ffe.12608